第 36 卷第 6 期
2017 年 12 月

红外与毫米波学报
J. Infrared Millim. Waves

Vol. 36, No. 6
December, 2017

文章编号: 1001 - 9014(2017)06 - 0673 - 07

DOI:10.11972/j.issn.1001 - 9014.2017.06.007

The sensitivity of mirrored aperture synthesis millimeter-wave radiometry

CHEN Liang-Bing*, WANG Yu-Hao, ZHOU Hui-Lin

(School of Information Engineering, Nanchang University, Nanchang 330031, China)

Abstract: Mirrored aperture synthesis (MAS) has been proposed to utilize a few antennas to provide high spatial resolution for Earth remote sensing. But the sensitivity of MAS is not completely analyzed. For this problem, the characteristic of the noise in 2-D MAS is derived. Further, both the sensitivity of 1-D and 2-D MAS are analyzed. Numerical simulations are carried out to evaluate the sensitivity of a MAS system, and comparisons between the sensitivity of MAS and traditional aperture synthesis are made.

Key words: aperture synthesis, mirrored aperture synthesis, sensitivity

PACS: 42.68.Wt, 84.40.-x

镜像综合孔径毫米波辐射测量灵敏度

陈良兵, 王玉皞, 周辉林

(南昌大学 信息工程学院,江西 南昌 330031)

摘要:镜像综合孔径可利用较少的天线获得地球遥感所需的高空间分辨率,但是镜像综合孔径辐射测量灵敏度尚未得到深入分析.针对该问题,推导了二维镜像综合孔径辐射测量噪声特性,在此基础上,对一维/二维镜像综合孔径测量灵敏度进行了分析,开展了仿真实验,并与常规综合孔径测量灵敏度进行了分析比较.

关 键 词:综合孔径;镜像综合孔径;灵敏度

中图分类号:TP722.6 **文献标识码**:A

Introduction

At present, passive millimeter-wave aperture synthesis radiometer is considered an atmospheric remote sensing technique from geostationary orbit[1-2]. But for a large aperture synthesis radiometer, it is always composed of large numbers of antennas, receivers, and correlators. The system is very complicated and difficult to be implemented. Thus how to reduce the system complexity is of great importance. And in Refs. [3-4], mirrored aperture synthesis (MAS) was proposed. It is based on a new system model with the combination of the two-element interferometers and Lloyd's mirror interferometers. Compared with traditional aperture synthesis, MAS can utilize an array with fewer elements to provide high spatial resolution for Earth remote sensing.

Some work has been done for MAS. The concept of 1-D and that of 2-D MAS were presented in Refs. [3-4] respectively. The proper antenna array for MAS was discussed in Refs. [5-6]. And the experiment system for MAS was introduced in Refs. [7]. But up to now, the sensitivity of 1-D MAS was only briefly derived in Refs. [3]. There were no further discussion about the ideal sensitivity and the actual sensitivity, no simulation for the sensitivity, and no comparison between the 1-D MAS and 1-D traditional aperture synthesis. The sensitivity of 2-D MAS has not been studied at all.

This paper is dedicated to the sensitivity of MAS. First, the principle of MAS is briefly introduced. Then, the derivations for the variance and the covariance of the cross-correlations between the signals collected by pairs of antennas are presented, especially for the 2-D case. Based on it, the covariance of the cosine visibility and that of reconstructed brightness temperature are derived, and the sensitivity under ideal case is discussed. Finally, in order to make detail comparisons, numerical simulations for the sensitivity of aperture synthesis and MAS

Received date: 2017-08-15, **revised date**: 2017-11-06 **收稿日期**:2017-08-15, **修回日期**:2017-11-06

Foundation items: Supported by National Natural Science Foundation of China (NSF41505015); Science Foundation of the Department of Science & Technology of Jiangxi Province (20151BAB213034); China Postdoctoral Science Foundation (2016M602085).

Biography: Chen Liang-Bing (1982-), male, Nanchang, Doctor. Research area involves millimeter-wave imaging for remote sensing and target detection.

* **Corresponding author**: E-mail: chenliangxiong1@163.com

are carried out.

1 Fundamentals of MAS

For MAS and aperture synthesis, a pair of antennas forms an interferometer, and the cross-correlation between the signals collected by antennas is the basic measurement. For 1-D MAS, the cross-correlation is[3]

$$R_{ij} = \langle b_i(t) b_j(t) \rangle = C_V(y_j - y_i) - C_V(y_j + y_i) \quad . \quad (1)$$

And for the 2-D MAS, the cross-correlation is[4]

$$R_{ij} = C_V(x_j - x_i, y_j - y_i) - C_V(x_j - x_i, y_j + y_i) - C_V(x_j + x_i, y_j - y_i) + C_V(x_j + x_i, y_j + y_i) \quad , \quad (2)$$

where (x_i, y_i) and (x_j, y_j) are the normalized coordinate of the two antennas with respect to wavelength λ, $C_V(v)$ and $C_V(u, v)$ are the 1-D cosine visibility and 2-D cosine visibility respectively given as

$$C_V(v) = 2\int_0^1 \frac{T_\Omega(\eta)}{\sqrt{1-\eta^2}} \cos(2\pi v \eta) \mathrm{d}\eta$$
$$C_V(u,v) = 4\int_0^1 \int_0^1 \frac{T_\Omega(\xi,\eta)}{\sqrt{1-\xi^2-\eta^2}} \cos(2\pi u \xi) \cos \mathrm{d}\xi \mathrm{d}\eta \quad , \quad (3)$$

where $(\xi, \eta) = (\sin\theta\cos\varphi, \sin\theta\sin\varphi)$ are the directional cosines, $T_\Omega(\eta)/\sqrt{1-\eta^2}$ and $T_\Omega(\xi,\eta)/\sqrt{1-\xi^2-\eta^2}$ are the 1-D and 2-D modified brightness temperature (BT) respectively, and (u, v) denotes the baseline (spatial frequency) depending on the antenna position difference.

One can obtain the corresponding equation similar to Eqs. 1-2 for each pair of elements in the array, and these equations can be combined to form linear equation sets expressed in matrix form. For example, for 2-D MAS, one has

$$\begin{bmatrix} R_{12} \\ R_{13} \\ \vdots \\ R_{(S-1)S} \end{bmatrix} = \begin{bmatrix} 1 & -1 & 0 & \cdots & 1 & 0 \\ \vdots & \vdots & \ddots & \cdots & \cdots & \vdots \\ 0 & \vdots & \vdots & \ddots & \cdots & \vdots \\ 0 & 1 & -1 & \cdots & -1 & 1 \end{bmatrix} \begin{bmatrix} C_V(0,1) \\ C_V(0,2) \\ \vdots \\ C_V(M,N) \end{bmatrix}$$
$$\overline{R} = \overline{\overline{P}} \; \overline{C_V} \quad , \quad (4)$$

where S is the number of elements in the array, M and N are the number of baselines along the two dimension respectively. According to Eq. 2, each row in the matrix $\overline{\overline{P}}$ contains only four non-zero elements, where two elements are with the value of 1, and other two elements are with the value of -1. And the positions of the four non-zero elements are determined by the corresponding indexes of the four spatial frequencies in the vector $\overline{C_V}$.

The linear equations can be solved by Pseudo-inverse method or common regularized inversion methods, such as Truncated Singular Value Decomposition (TSVD) and Tikhonov regularization[8], to obtain the estimation of the cosine visibilities. The solution can be generally written as follows:

$$\overline{C_V} = \overline{\overline{A}}\, \overline{R} \quad , \quad (5)$$

where the matrix $\overline{\overline{A}}$ is determined by the matrix $\overline{\overline{P}}$ and the inversion method. Then by 1-D inverse cosine transform or 2-D inverse cosine transform, the BT image can be reconstructed. The inverse cosine transform can be written as a matrix representation, given as

$$\overline{T} = \overline{\overline{B}}\, \overline{C_V} \quad , \quad (6)$$

where $\overline{\overline{B}}$ is the corresponding 1-D or 2-D cosine transform matrix.

2 The sensitivity of MAS

The cross-correlations are with noise because of the finite integration time. The variance and the covariance of the cross-correlations for 1-D MAS are derived in Ref. [3]. The derivation process for 2-D MAS is shown in Appendix (see (A.6) and (A.9)), which is similar to that in Ref. [3]. And it is found that the expressions of the variance and the covariance for 2-D MAS are the same as those for 1-D MAS. The expressions are given as

$$\langle \Delta R_{ij}^2 \rangle = \frac{1}{2B\tau}(R_{ii}R_{jj} + R_{ij}^2)$$
$$\langle \Delta R_{ij} \Delta R_{kl} \rangle = \frac{1}{2B\tau}(R_{ik}R_{jl} + R_{il}R_{jk}) \quad , \quad (7)$$

where $\langle \Delta R_{ij}^2 \rangle$ denotes the variance, $\langle \Delta R_{ij} \Delta R_{kl} \rangle$ denotes the covariance, B is the bandwidth, and τ is the integration time. Contrastively, the variance and the covariance of the visibilities for aperture synthesis are[9]

$$\langle \Delta V_{ij} \Delta V_{ij}^* \rangle = \frac{1}{B\tau} V_{ii} V_{jj}^*$$
$$\langle \Delta V_{ij} \Delta V_{kl}^* \rangle = \frac{1}{B\tau} V_{ik} V_{jl}^* \quad . \quad (8)$$

The covariance matrix $\overline{\overline{\Gamma_R}}$ on the cross-correlations for MAS can be defined by Eq. 7. Let $\overline{\overline{\Gamma_{CV}}}$ denote the covariance matrix on the cosine visibilities, and it can be obtained from Eq. 5, given as

$$\overline{\overline{\Gamma_{CV}}} = \overline{\overline{A}}\, \overline{\overline{\Gamma_R}} (\overline{\overline{A}})^{\mathrm{T}} \quad , \quad (9)$$

where the superscript T represents the matrix transpose. Similarly, the covariance matrix on BT can be obtained from Eq. 6 and Eq. 9, given as

$$\overline{\overline{\Gamma_T}} = \overline{\overline{B}}\, \overline{\overline{\Gamma_{CV}}}\, \overline{\overline{B}}^{\mathrm{T}} = \overline{\overline{B}}\, \overline{\overline{A}}\, \overline{\overline{\Gamma_R}} (\overline{\overline{B}}\, \overline{\overline{A}}^{\mathrm{T}}) \quad . \quad (10)$$

Each element in the diagonal of $\overline{\overline{\Gamma_T}}$ is the variance of the noise at each pixel. The standard derivation of the noise, i.e. the square root of the variance, is the sensitivity at each pixel.

Because the Eqs. 5, 9-10 are all numeric, an analytic expression for the sensitivity is generally impossible. But considering an extremely ideal case, the optimal sensitivity of MAS can be derived as follows.

(a) According to Eq. 1 and considering the receiver noise temperature T_r, R_{ii} can be expressed as

$$R_{ii} = C_V(0) - C_V(2y_i) + T_r \quad . \quad (11)$$

Generally, the magnitude of cosine visibility at the zero baseline is much greater than that at the long baseline. Thus, R_{ii} can be approximate to

$$R_{ii} \approx C_V(0) + T_r = T_{sys} \quad . \quad (12)$$

Similarly according to (2), for 2-D MAS:

$$R_{ii} \approx C_V(0,0) + T_r = T_{sys} \quad . \quad (13)$$

(b) When observing the Earth by millimeter-wave instrument, the receiver noise temperature is always high, and the cross-correlation is always small. Taking

GeoSTAR for example, the cross-correlation is smaller than 5K. So $R_{ii}R_{jj} >> R_{ij}^2$ holds. And the covariance between the cross-correlations is usually omitted, because it is much smaller than the variance in Earth remote sensing. Thus, Eq. 7 can be simplified as

$$\langle \Delta R_{ij}^2 \rangle \approx \frac{R_{ii}R_{jj}}{2B\tau} = \frac{T_{sys}^2}{2B\tau} \qquad (14)$$
$$\langle \Delta R_{ij} \Delta R_{kl} \rangle \approx 0$$

Similarly for traditional aperture synthesis, the variance and the covariance of the visibilities can be simplified as

$$\langle \Delta V_{ij} \Delta V_{ij}^* \rangle = \frac{T_{sys}^2}{B\tau} \qquad (15)$$
$$\langle \Delta V_{ij} \Delta V_{kl}^* \rangle \approx 0$$

I/Q demodulation is necessary in traditional aperture synthesis while it is not needed in MAS. This is why there is a factor of 2 in the denominator in Eq. 14 but none in Eq. 15.

(c) It is assumed that the linear equations relating the cross-correlations and the cosine visibilities are well posed, and the cosine visibilities are independent and with the same variance. Then, according to Eq. 1, the variance of cosine visibilities for 1-D MAS is

$$\langle \Delta CV^2(v) \rangle = \frac{1}{2}\langle \Delta R_{ij}^2 \rangle = \frac{T_{sys}^2}{4B\tau} \qquad (16)$$

And according to (2), the variance for 2-D MAS is

$$\langle \Delta CV^2(u,v) \rangle = \frac{1}{4}\langle \Delta R_{ij}^2 \rangle = \frac{T_{sys}^2}{8B\tau} \qquad (17)$$

Thus, under ideal case, the variance of the cosine visibilities in Eq. 16 for 1-D MAS is a quarter of that in Eq. 15 for 1-D aperture synthesis. And for 2-D MAS, the variance of the cosine visibilities in Eq. 17 is one-eighth of that for 2-D aperture synthesis.

(d) For aperture synthesis, the BT image is reconstructed by Fourier transform from the visibility. Because discrete Fourier transform preserves the second norm, the total noise in the reconstructed BT image equals to the total noise in the visibility samples. Thus, the average noise power of the BT image for aperture synthesis is[9]

$$\Delta T_{avg}^2 = \frac{1}{N_V}\sum_m \sum_n |\Delta T(m,n)|^2 = \frac{T_{sys}^2}{B\tau}N_v \quad , \qquad (18)$$

where $|\Delta T(m,n)|^2$ denotes the noise power at pixel (m,n), and N_V is the number of the sampling frequencies for aperture synthesis. Here, the root-mean square (RMS) sensitivity is defined as the root square of the average noise power and denoted by ΔT_{RMS}. Thus, for aperture synthesis, the RMS sensitivity is:

$$\Delta T_{PMS}^{IAS} = \frac{T_{sys}}{\sqrt{B\tau}}\sqrt{N_V} \qquad (19)$$

Deferent from the sensitivity at each pixel, the RMS sensitivity is independent on the covariance between the visibilities.

For MAS, the BT image is retrieved by inverse cosine transform from the cosine visibilities. And since the cosine transform is a special case of the Fourier Transform, the RMS sensitivity for MAS is similarly to Eq. 18. For 1-D MAS:

$$\Delta T_{RMS}^{1D} = \sqrt{\Delta T_{avg}^2} = \frac{T_{sys}}{2\sqrt{B\tau}}\sqrt{N_{CV}} \qquad (20)$$

For 2-D MAS:

$$\Delta T_{RMS}^{2D} = \sqrt{\Delta T_{avg}^2} = \frac{T_{sys}}{2\sqrt{2}\sqrt{B\tau}}\sqrt{N_{CV}} \quad . (21)$$

where N_{CV} is the total number of the sampling frequencies for MAS. Considering the same bandwidth, the same integration time, and the same number of the sampling frequencies, the optimal sensitivity of 1-D MAS will be a half of the sensitivity of 1-D aperture synthesis, and the optimal sensitivity of 2-D MAS will be $1/2\sqrt{2}$ of the sensitivity of 2-D aperture synthesis. But for MAS, there are two main obstacles to obtain the optimal sensitivity:

(a) Because the cosine visibilities should be firstly solved from Eq. 1, the algorithm applied to obtain the cosine visibilities will has a great impact on the sensitivity. In particular, when Eq. 1 is not well posed, the noise in the cross-correlations will be amplified during the signal processing, and the optimal sensitivity cannot be obtained.

(b) MAS can utilize a small array to obtain a high spatial resolution by combining several measurements. Thus the integration time for each measurement will be shorter, and the optimal sensitivity cannot be obtained.

The impact of these factors is difficult to be evaluated by analytic analysis. The actual sensitivity of MAS can only be evaluated by numeric simulation. And detail comparisons between the sensitivity of MAS and aperture synthesis can be made by numeric simulation.

3 Comparisons between the sensitivity of MAS and aperture synthesis by numerical simulation

3.1 Comparisons between 1-D MAS and aperture synthesis

The array for 1-D MAS is a 12-element array with the normalized antenna spacing {6, 6, 6, 6, 6, 4, 2, 1, 1, 1, 2}. Two measurements are taken, and the linear equations are combined to provide the spatial frequency coverage without baseline missing and the matrix $\overline{\overline{P}}$ in Eq. 4 with a proper rank. One measurement is taken at the distance of 3λ from the array to the reflector with the normalized antenna coordinates {3, 9, 15, 21, 27, 33, 37, 39, 40, 41, 42, 44}, and the other is at the distance of 5λ with the normalized antenna coordinates {5, 11, 17, 23, 29, 35, 39, 41, 42, 43, 44, 46}. The two measurements provide the longest baseline of 90λ.

The array for 1-D aperture synthesis is a low-redundancy linear array of 16 elements with the normalized antenna spacing {1, 1, 6, 6, 6, 11, 11, 11, 11, 11, 5, 5, 3, 1, 1}, and it also provides the longest baseline of 90λ[10]. With the same spatial resolution, the sensitivity of 1-D MAS and 1-D aperture synthesis can be simulated and compared.

Due to the shortest baseline of one wavelength, the field of view is from $-\pi/6$ to $\pi/6$. And the antenna pattern is set as an ideal fan beam pattern

$$F_n(\theta,\phi) = \begin{cases} 1 & \text{for } |\pi/2-\theta| < \Delta\theta, |\phi| < \pi/6 \\ 0 & \text{otherwise} \end{cases} \quad , \qquad (22)$$

where $\Delta\theta$ is the narrow beamwidth of the fan beam. The scene to be imaged is with a stepped uniform BT as

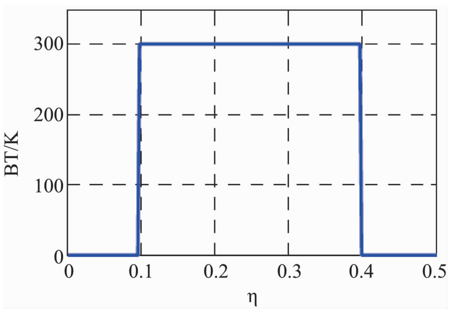

Fig. 1 The scene to be imaged, a stepped uniform BT of 300 K

图 1 成像场景,亮温为 300 K 的阶梯分布展源

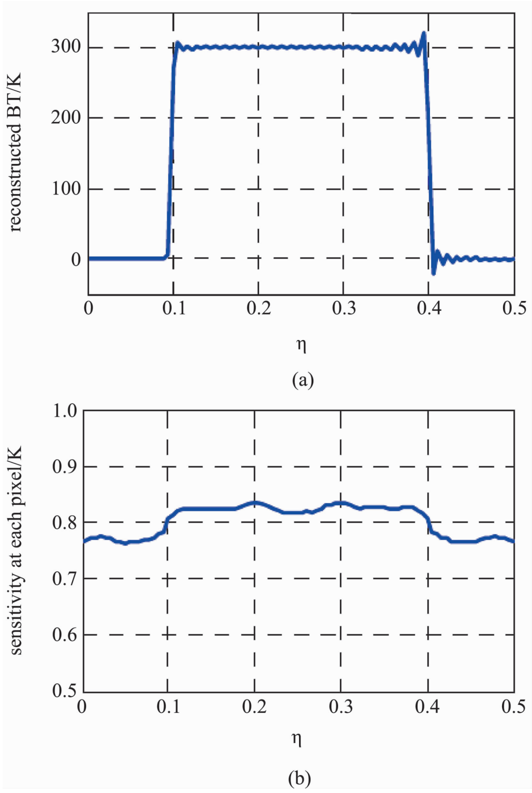

Fig. 2 The simulated results for 1 – D aperture synthesis: (a) The reconstructed BT, (b) the sensitivity at each pixel

图 2 一维综合孔径仿真结果(a)重建亮温分布,(b)各像素点灵敏度

shown in Fig. 1. The bandwidth is set to be 100 MHz. The integration time for 1-D aperture synthesis is set to be 1 s. The integration time for each MAS measurement is set to be 0.5 s, and the total measurement time is 1s. The receiver noise temperature is set to be 500 K.

For 1-D aperture synthesis, the covariance of the reconstructed BT is computed by Eq. 8. The simulated results are shown in Fig. 2 (in order to be convenient to compare, only the positive part of the view field displayed), where Fig. 2(a) is the reconstructed BT and Fig. 2(b) is the sensitivity at each pixel. Since the correlation between visibilities is taken into account, the

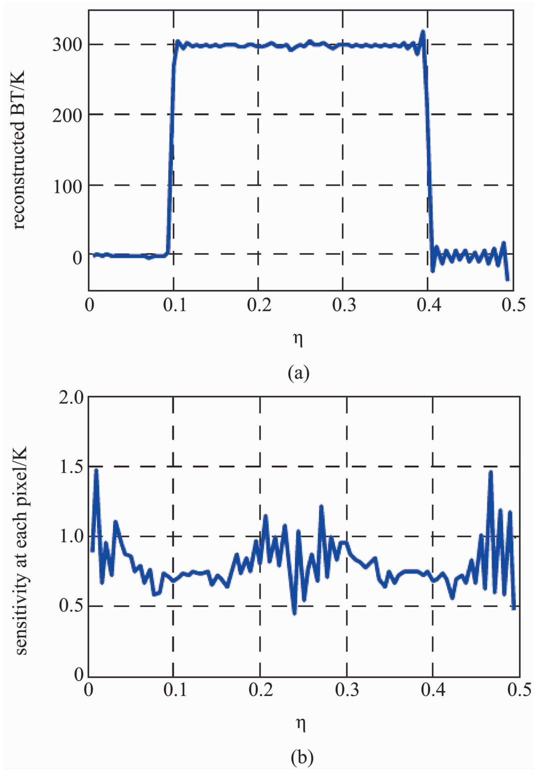

Fig. 3 The simulated results for 1-D MAS (a) the reconstructed BT by TSVD, (b) the sensitivity at each pixel by TSVD

图 3 一维镜像综合孔径仿真结果(a)利用 TSVD 重建的亮温分布,(b) 利用 TSVD 重建得到的各像素点灵敏度

sensitivity of 1-D aperture synthesis follows the distribution of the scene, which matches well the discussion in Ref. [11]. The RMS sensitivity ΔT_{PMS}^{LAS} of the system is about 0.8 K.

For 1-D MAS, the covariance matrix of the cross-correlations is computed by Eq. 7, and the covariance of the reconstructed BT is computed by Eq. 9. TSVD is applied to obtaining the cosine visibilities from Eq. 4. The number of singular values of $\overline{\overline{P}}$ is 90, but only 84 greatest singular values of $\overline{\overline{P}}$ are kept for TSVD. Other smaller singular values are abandoned. Fig. 3(a) is the reconstructed BT image by TSVD. Fig. 3(b) is the corresponding sensitivity at each pixel, and the RMS sensitivity is about 0.82 K, which is approximate to the RMS sensitivity of the aperture synthesis system. But according to Eq. 16, the optimal RMS sensitivity is about 0.4 K, which is a half of the sensitivity of the 1-D aperture synthesis system. It shows that the noise in the cross-correlation is amplified, which causes 1-D MAS cannot reach the optimal sensitivity.

3.2 Comparisons between 2-D MAS and aperture synthesis

The 2-D array for 2-D MAS contains 36 antenna elements. Each row and column of the 2-D array is a 6-element linear array with normalized antenna spacing {4, 3, 1, 1, 1}, as shown in Fig. 4. Similarly, two measurements are taken and combined. One measurement is taken at the distance of 2λ from the array to the two reflectors (shown in Fig. 4(a)), and the other is at the distance of 3λ from the array to the two reflectors (shown in Fig. 4(b)). The two measurements provide the longest baseline of 26λ at both dimensions. The integration time for each MAS measurement is set to be 0.5 s, and the total measurement time is 1 s.

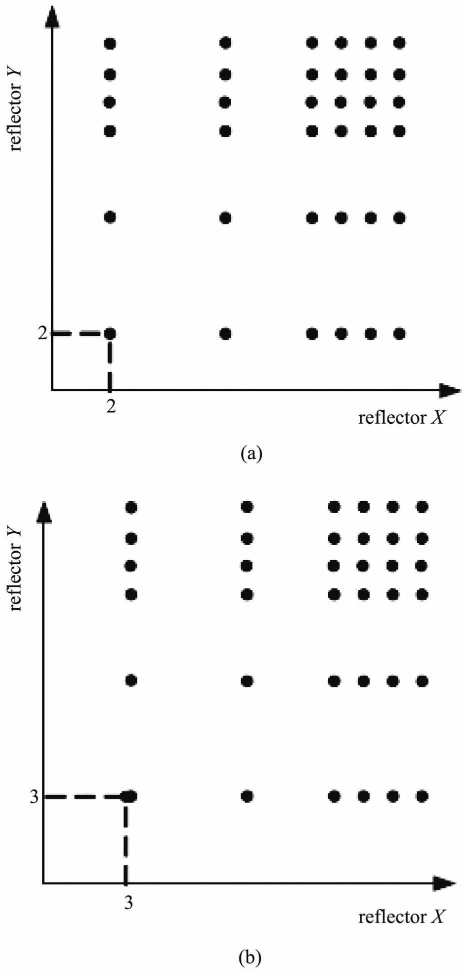

Fig. 4　The array arrangement for 2-D MAS (a) The distance of 2λ from the array to the reflectors, (b) the distance of 3λ from the array to the reflectors
图 4　二维镜像综合孔径天线排布(a)阵列到反射面距离为 2λ 时,(b)阵列到反射面距离为 3λ 时

The array for 2-D aperture synthesis is arranged as the shape of "U" with 27 antennas in each arm, totally 79 antennas. The minimum antenna element spacing between adjacent antennas is one wavelength (λ). The array also provides the longest baseline of 26λ along both the dimensions.

The scene to be imaged is with a stepped uniform BT as shown in Fig. 5. The other system parameters are the same as the 1-D case.

The simulated results for 2-D aperture synthesis are shown in Fig. 6 (only the positive part of the view field displayed), where Fig. 6(a) is the reconstructed BT and Fig. 6(b) is the sensitivity at each pixel. It's also found

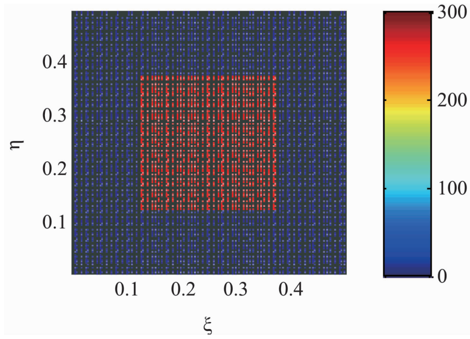

Fig. 5　The 2-D scene to be imaged, a stepped uniform BT of 300 K
图 5　二维成像场景,亮温为 300 K 的阶梯分布展源

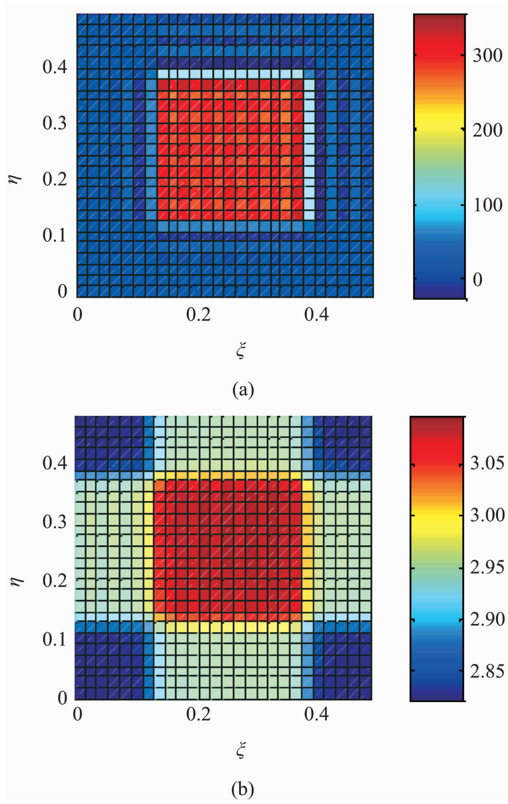

Fig. 6　The simulated results for 2-D aperture synthesis (a) The reconstructed BT, (b) the sensitivity at each pixel
图 6　二维综合孔径仿真结果(a)重建亮温分布,(b)各像素点灵敏度

that the sensitivity of 2-D aperture synthesis follows the distribution of the scene. The RMS sensitivity of the system is about 2.89 K.

The simulated results for 2-D MAS are shown in Fig. 7. The number of singular values of is 550, but only the 530 greatest singular values of are kept for TSVD. Fig. 7(a) is the reconstructed BT image by TSVD. Fig. 7(b) is the corresponding sensitivity at each pixel, and the RMS sensitivity is about 1.99 K, which is smaller than the RMS sensitivity of the aperture synthesis system. But the RMS sensitivity is still much greater than

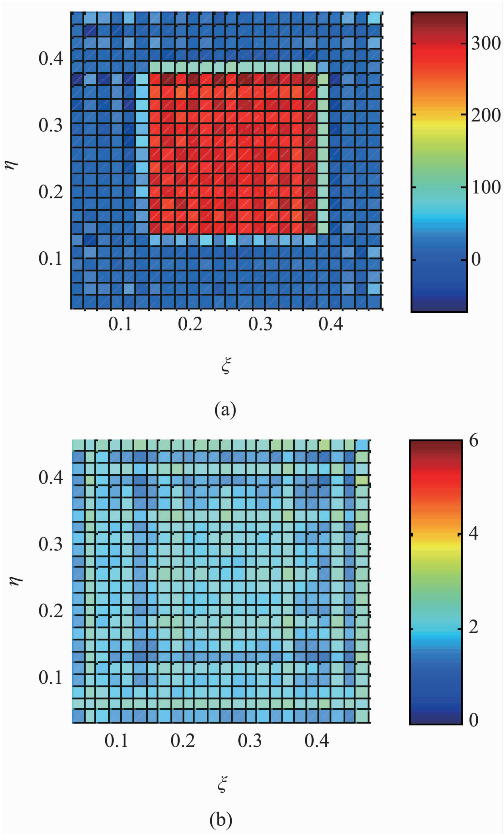

Fig. 7 The simulated results for 2-D MAS (a) The reconstructed BT by TSVD, (b) the sensitivity at each pixel by TSVD
图7 二维镜像综合孔径仿真结果(a)利用TSVD重建的亮温分布,(b)利用TSVD重建得到的各像素点灵敏度

the optimal sensitivity of about 1.02 K, which is of the sensitivity of the 2-D aperture synthesis system.

4 Conclusions

In this paper, the sensitivity of MAS is analyzed and compared with that of aperture synthesis. Because I/Q demodulation is not required in MAS, the variance of the cross-correlation for MAS is a half of that for aperture synthesis, and the optimal sensitivity of MAS is superior to that of aperture synthesis under the ideal case. But the actual sensitivity of MAS highly depends on the algorithm applied to solve the linear equations, and generally due to the impact of the algorithm, MAS cannot reach the optimal sensitivity.

Compared with aperture synthesis, MAS is still premature. There is a long way to go from the study to a mature concept design, a prototype, and practical application. More work is needed, such as antenna array design, calibration, image reconstruction algorithms, the impact of system imperfections on the accuracy, the error budget, the impact of polarization and so on. We will solve these problems one by one in the following study, and then develop a small prototype to demonstrate the feasibility of MAS sufficiently. After these work, we will aim at the geostationary atmospheric sounding and do further work.

Appendix: The Variance and the Covariance of the Cross-correlation for 2-D MAS

The process of derivation for 2-D MAS is similar to that for 1-D MAS in Ref. [4], and a brief derivation is presented here. First, the autocorrelation is established based on the system model and the signal model. Then the variance and the covariance are derived respectively.

The detail model for a 2-D MAS system is presented in Ref. [4]. Each antenna collects four signals emitted from the source, given as

$$b_i(t) = b_i^d(t) + b_i^x(t) + b_i^y(t) + b_i^o(t) \quad , \quad (A.1)$$

where the superscript d, x, y, and o denote the direct signal and reflected signals collected by the antenna respectively. The output of each receiver contains not only the signal but also the receiver noise denoted by $n(t)$. Then the multiplication of two signals before entering the integrators is

$$m_{ij}(t) = [b_i(t) + n_i(t)][b_j(t) + n_j(t)] \quad . \quad (A.2)$$

The autocorrelation is given as

$$\begin{aligned} R_{m_{ij}} &= < m_{ij}(t) m_{ij}(t+\tau) > \\ &= < b_i(t) b_j(t) >^2 + < b_i(t) b_i(t+\tau) > \cdot < b_j(t) b_j(t+\tau) > \\ &+ < b_i(t) b_i(t+\tau) > \cdot < n_j(t) n_j(t+\tau) > \\ &+ < b_j(t) b_j(t+\tau) > \cdot < n_i(t) n_i(t+\tau) > \\ &+ < n_i(t) n_i(t+\tau) > \cdot < n_j(t) n_j(t+\tau) > \\ &+ < b_i(t) b_j(t+\tau) > \cdot < b_j(t) b_i(t+\tau) > \quad , \quad (A.3) \end{aligned}$$

where < > denotes the ensemble average. And one has

$$\begin{aligned} < b_i(t) b_j(t+\tau) > &= < [b_i^d(t) + b_i^x(t) + b_i^y(t) + b_i^o(t)] \\ &\cdot [b_j^d(t+\tau) + b_j^x(t+\tau) + b_j^y(t+\tau) + b_j^o(t+\tau)] > \\ &= \mathrm{sinc}(B\tau)\cos(2\pi f_c \tau) R_{ij} \quad . \quad (A.4) \end{aligned}$$

Equation (A.4) can be applied to any combination (i, j), for example:

$$< b_i(t) b_i(t+\tau) > = \mathrm{sinc}(B\tau)\cos(2\pi f_c\tau)(R_{ii} - T_i^{rec})$$

$$< n_i(t) n_i(t+\tau) > = T_i^{rec}\mathrm{sinc}(B\tau)\cos(2\pi f_c\tau)$$

where T_i^{rec} is the equivalent noise temperature of the receiver.

The results can be substituted into Eq. (A.3), and the high frequency term with $\cos(4\pi f_c t)$ in the autocorrelation can be filtered by the integrators, because integrators can be regarded as a low-pass filter. Thus, one obtains:

$$R_{m_{ij}}(\tau) = R_{ij}^2 + \frac{1}{2}\mathrm{sinc}^2(B\tau)(R_{ii}R_{jj} + R_{ij}^2) \quad . \quad (A.5)$$

Then the variance of the cross-correlations in 2-D MAS is:

$$< \Delta R_{ij}^2 > = \frac{1}{2B\tau}(R_{ii}R_{jj} + R_{ij}^2) \quad . \quad (A.6)$$

The cross-correlation of the process is given as

$$\begin{aligned} R_{m_{ij}}(\tau) &= < m_{ij}(t) m_{kl}(t+\tau) > \\ &= < [b_i(t) + n_i(t)][b_j(t) + n_j(t)] \\ &\cdot [b_k(t+\tau) + n_k(t+\tau)][b_l(t+\tau) + n_l(t+\tau)] > \quad . \quad (A.7) \end{aligned}$$

Similar to that in Ref. [13], the expected values of 15 products in Eq. (A.7) are zero, and only one product is nonzero.

$$R_{m_{ij}m_{kl}}(\tau) = < b_i(t)b_j(t) \cdot b_k(t+\tau)b_l(t+\tau) > = R_{ij}R_{kl} + \frac{1}{2}\mathrm{sinc}^2(B\tau)(R_{ik}R_{jl} + R_{il}R_{jk}) \quad . \quad (A.8)$$

Then, the covariance of cross-correlations for 2-D MAS is:

$$< \Delta R_{ij}\Delta R_{kl} > = \frac{1}{2B\tau}(R_{ik}R_{jl} + R_{il}R_{jk}) \quad . \quad (A.9)$$

References

[1] Zhang Y, Liu H, Wu J, *et al*. Analysis and simulation of GIMS observation on dynamic targets[C]. *Geoscience and Remote Sensing Symposium. IEEE*, 2016: 426-429.

[2] HU An-Yong, BAI Ming, MIAO Jun-Gang. Optic real-time signal processing for synthetic aperture microwave radiometer[J]. *J. Infrared Millim. Waves* (胡岸勇, 白明, 苗俊刚. 综合孔径微波辐射计光学实时信号处理系统. **红外与毫米波学报**), 2012, **31**(4): 348-354.

[3] Chen L, Li Q, Yi G, and Zhu Y. 1-D mirrored interferometric aperture synthesis: performances, simulation, and experiments[J]. *IEEE Tran. Geosci. Remote Sens.*, 2013, **51**(5): 2960-2968.

[4] Chen L and Zhang X. 2-D mirrored interferometric aperture synthesis [C]. ISAPE2012, 2012: 482-485.

[5] Zhu D, Hu F, Wu L, Li J, and Lang L. Low-redundancy linear arrays in mirrored interferometric aperture synthesis[J]. *Optics Letters*, 2015, **41**(2): 368-371.

[6] Li Y, Li Q, Jin R, *et al*. Array configuration optimization for Rotating mirrored aperture synthesis (RMAS)[C]. IEEE International Geoscience and Remote Sensing Symposium (*IGARSS*), 2016: 853-856.

[7] Li Q, Chen K, Guo W, *et al*. ESMAS: experiment system of mirrored aperture synthesis [C]. *IEEE International Geoscience and Remote Sensing Symposium* (*IGARSS*), 2016: 2028-2031.

[8] Bertero M and Boccacci P. *Introduction to Inverse Problems in Imaging* [M]. London, U.K.: Inst. Physics, 1998.

[9] Butora R and Camps A, Noise maps in aperture synthesis radiometric images due to cross-correlation of visibility noise[J]. *Radio Science*, 2003, **38**(4): 1067-1074.

[10] Dong J, Li Q, Zhu Y, *et al*. A method for seeking low-redundancy large linear arrays in aperture synthesis microwave radiometers[J]. *IEEE Tran. Antennas. Propagat.*, 2010, **58**(6): 1913-1921.